Supplementary Material

Self-supporting 3D hierarchically porous CuNi-S cathodes with dual-phase structure for rechargeable Al battery

Aijing Lv[a], Songle Lu[a], Wenjing Yan[a], Wentao Hu[c,], Mingyong Wang[a,b,]**

[a]State Key Laboratory of Advanced Metallurgy, University of Science and Technology Beijing, Beijing 100083, P R China

[b]Beijing Key Laboratory of Green Recovery and Extraction of Rare and Precious Metals, University of Science and Technology Beijing, Beijing 100083, China

[c]School of Civil and Resource Engineering, University of Science and Technology Beijing, 100083 Beijing, P. R. China.

Corresponding author. Tel & Fax: 86-010-82376882, E-mail: wthu010@ustb.edu.cn (W T Hu), mywang@ustb.edu.cn (M Y Wang)

Table of Contents

Table S1. Electrolyte compositions for metal electrodeposition based on different Cu/Ni ratio.

Cu/Ni ratio	Electrolyte compositions				
	$CuSO_4$ (M)	**$NiSO_4$ (M)**	**$(NH_4)_2SO_4$ (M)**	**H_2SO_4 (M)**	**SDS (mM)**
1:0	0.1	--	1.0	0.7	1.0
1:1	0.1	0.1	1.0	0.7	1.0
1:2	0.1	0.2	1.0	0.7	1.0
0:1	--	0.1	1.0	0.7	1.0

Table S2. Cathodes names for the self-supporting cathodes based on different Cu/Ni ratio.

Cu/Ni ratio	Cathodes name		
	Electrodeposited Samples	**Oxidation Samples**	**Sulfur Replacement Samples**
1:0	Cu/CC	Cu-O/CC	Cu-S/CC
1:1	$CuNi/CC_{1.0}$	$CuNi\text{-}O/CC_{1.0}$	$CuNi\text{-}S/CC_{1.0}$
1:2	$CuNi/CC_{2.0}$	$CuNi\text{-}O/CC_{2.0}$	$CuNi\text{-}S/CC_{2.0}$
0:1	Ni/CC	Ni-O/CC	Ni-S/CC

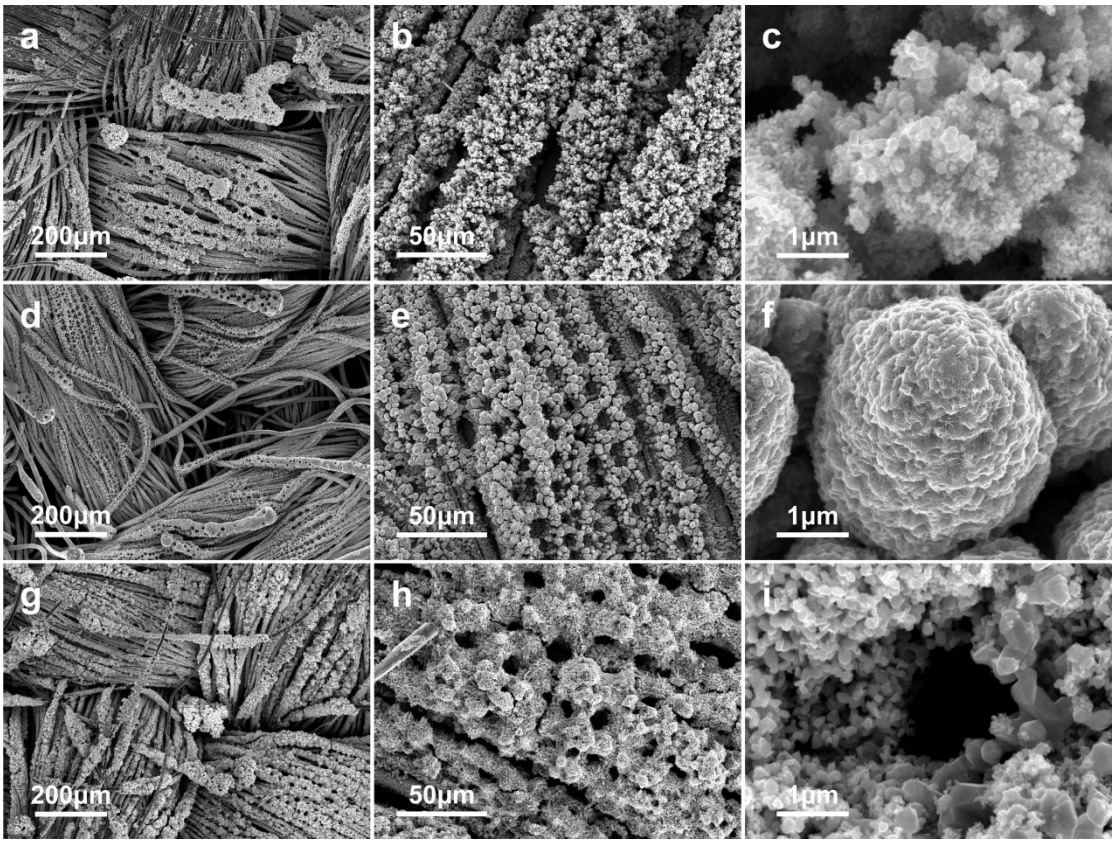

Fig. S1 SEM images of (a-c) Cu-S/CC, (d-f) Ni-S/CC and (g-i) CuNi-S/$CC_{2.0}$.

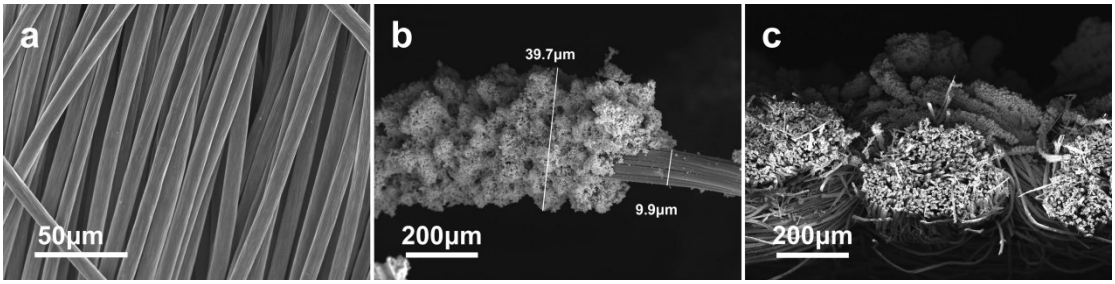

Fig. S2 SEM images of (a) carbon cloth (CC) fibers and (b) carbon fibers covered by CuNi-$S_{1.0}$. (c) Top-view SEM image of CuNi-S/$CC_{1.0}$.

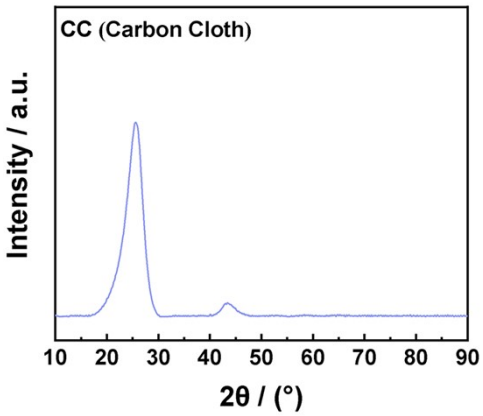

Fig. S3 XRD pattern of carbon cloth (CC) fibers.

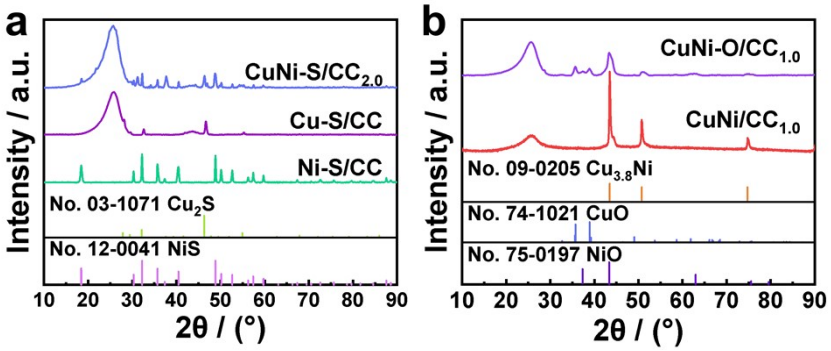

Fig. S4 (a) XRD patterns of Ni-S/CC, Cu-S/CC and CuNi-S/$CC_{2.0}$. (b) XRD patterns of CuNi/$CC_{1.0}$ and CuNi-O/$CC_{1.0}$.

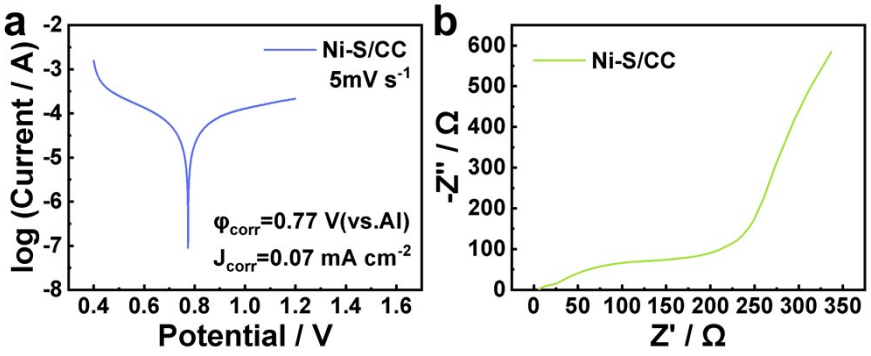

Fig. S5 Corrosion resistance and electrical conductivity of self-supporting Ni-S/CC cathode based on $AlCl_3$/[EMIm]Cl ionic liquids. (a) Tafel curves and electrochemical corrosion parameters of Ni-S/CC. (b) Nyquist plots of Ni-S/CC cathode before cycling.

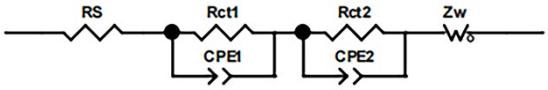

Fig. S6 Equivalent circuit for EIS of Cu-S/CC, Ni-S/CC, CuNi-S/$CC_{1.0}$, CuNi-S/$CC_{2.0}$, CuNi-O/$CC_{1.0}$ and CuNi/$CC_{1.0}$ cathodes.

Where *Rs* is the solution resistance; R_{ct1} and CPE_1 are the micro-pore resistance and constant phase element of various self-supporting cathodes; R_{ct2} and CPE_2 are the charge-transfer resistance and constant phase element of various self-supporting cathodes; Z_w is associated with the Warburg impedance.

Table S3. EIS parameters and diffusion coefficients obtained by fitting the impedance spectra of CuNi/$CC_{1.0}$, CuNi-O/$CC_{1.0}$, CuNi-S/$CC_{1.0}$, CuNi-S/$CC_{2.0}$, Cu-S/CC and Ni-S/CC cathodes

Parameter	CuNi/$CC_{1.0}$	CuNi-O/$CC_{1.0}$	CuNi-S/$CC_{1.0}$	CuNi-S/$CC_{2.0}$	Cu-S/CC	Ni-S/CC
R_s / Ω cm^2	4.33	5.50	4.25	5.09	5.05	4.96
R_{ct1} / Ω cm^2	6.84	6.52	4.24	2.64	5.90	11.30
$CPE_{1\text{-}T}$ / Ω^{-1} s^n cm^{-2}	9.95×10^{-5}	2.80×10^{-5}	1.96×10^{-5}	7.96×10^{-5}	3.79×10^{-4}	1.90×10^{-5}
$CPE_{1\text{-}P}$	0.66	0.77	0.77	0.73	0.59	0.92
R_{ct2} / Ω cm^2	73.98	409.90	126.50	108.90	225.50	88.06
$CPE_{2\text{-}T}$ / Ω^{-1} s^n cm^{-2}	2.89×10^{-4}	1.16×10^{-3}	1.35×10^{-3}	1.21×10^{-3}	4.89×10^{-4}	2.18×10^{-4}
$CPE_{2\text{-}P}$	0.79	0.64	0.69	0.74	0.71	0.86
$Z_{w\text{-}R}$ / Ω cm^2	919.80	60.97	36.46	29.97	39.64	411.40
$Z_{w\text{-}T}$	7.86	0.37	0.43	0.47	0.15	1.09
$Z_{w\text{-}P}$	0.56	0.39	0.43	0.37	0.34	0.47
σ	92.57	61.67	20.86	16.90	46.51	118.00
DC[a)] / cm^2 s^{-1}	9.49×10^{-16}	2.14×10^{-15}	1.87×10^{-14}	2.85×10^{-14}	3.76×10^{-15}	5.84×10^{-16}

[a)] The diffusion coefficient (DC) is calculated as follow:

$$DC = \frac{1}{2}\left[\frac{RT}{F^2 n^2 AC\sigma}\right]^2 \quad (S1)$$

$$Z_{re} = K + \sigma\omega^{-1/2} \quad (S2)$$

Where R is the gas constant(8.314 J K^{-1} mol^{-1}); T is the absolute temperature (298 K); F is the Faraday constant (96485 C mol^{-1}); n is the electron transfer number; A is the active surface area of the cathode (1 cm^2); C is the concentration of Al ions in the cathode electrode (~1.65×10^{-2} mol cm^{-3})； σ is the Warburg coefficient, determined by the slope of the real resistance Z_{re} vs. $\omega^{-1/2}$ in low frequency region ($\omega=2\pi f$).

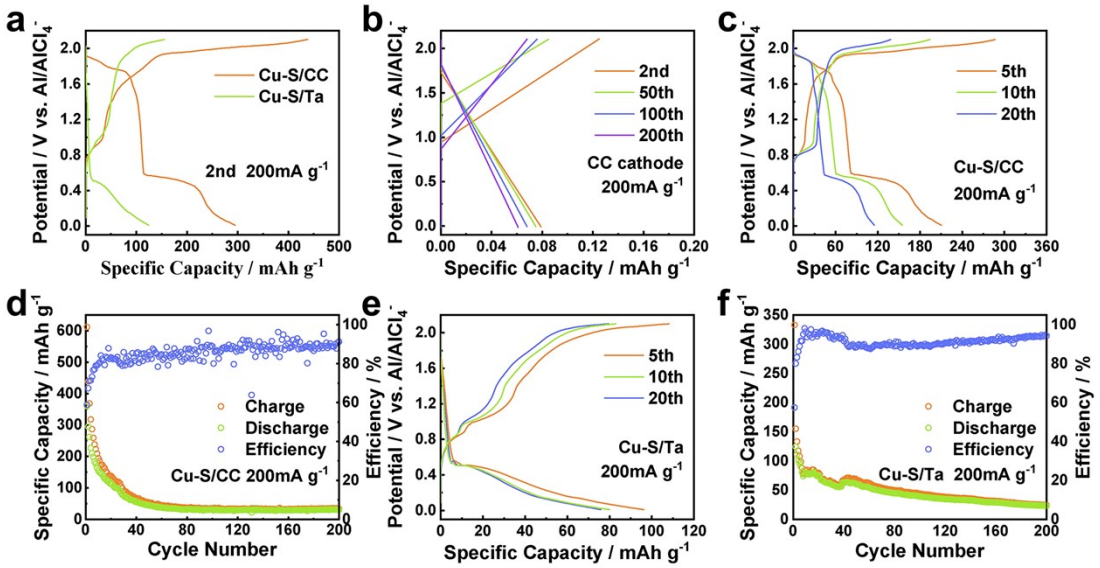

Fig. S7 (a) Charge/discharge curves of Cu-S/CC and powdery Cu-S/Ta cathode of 2nd cycle at the current densities of 200 mA g^{-1}. (b) Charge/discharge curves of 2nd, 5th, 100th, 200th cycles of CC cathode at a current density of 200 mA g^{-1}. Charge/discharge curves of 5th, 10th, 20th cycles of (c) Cu-S/CC, (e) powdery Cu-S/Ta cathode at a current density of 200 mA g^{-1}. Cycling performance and coulombic efficiency of (d) Cu-S/CC and (f) powdery Cu-S/Ta at a current density of 200 mA g^{-1}.

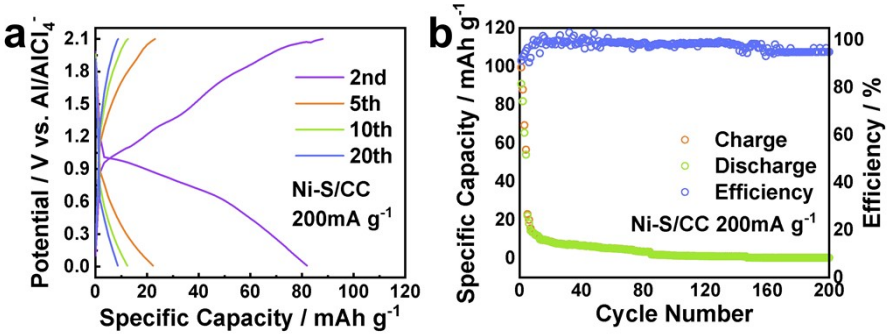

Fig. S8 (a) Charge/discharge curves of Ni-S/CC cathode for 2nd, 5th, 100th, 200th cycles at a current density of 200 mA g^{-1}. (b) Cycling performance and coulombic efficiency of Ni-S/CC at a current density of 200 mA g^{-1}.

Table S4. Comparison of loading mass and electrochemical performance of various self-supporting cathodes prepared in this paper for Al battery cathodes

Material	Loading mass / mg cm^{-2}	Cycle number	Initial capacity / mA h g^{-1}	Last capacity / mA h g^{-1}	Current Density / mA g^{-1}	Coulombic Efficiency / %
$CuNi/CC_{1.0}$	5.3	--	--	--	--	--
$CuNi\text{-}O/CC_{1.0}$	5.2	200	26.00	8.2	200	98.4
$CuNi\text{-}S/CC_{1.0}$	4.2	200	333.5	70.5	200	99.4
$CuNi\text{-}S/CC_{2.0}$	4.8	200	398.1	54.3	200	100.9
Cu-S/CC	2.2	200	294.8	30.0	200	91.3
Ni-S/CC	5.3	200	81.88	0.32	200	95.0
Cu-S/Ta	0.6	200	124.2	23.0	200	94.3

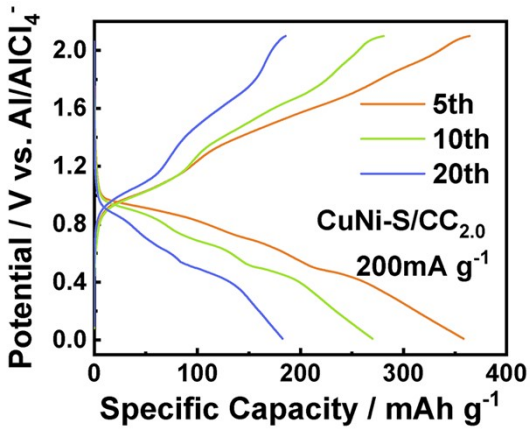

Fig. S9 Charge/discharge curves of CuNi-S/$CC_{2.0}$ cathode for 5th, 10th, 20th cycles at a current density of 200 mA g^{-1}.

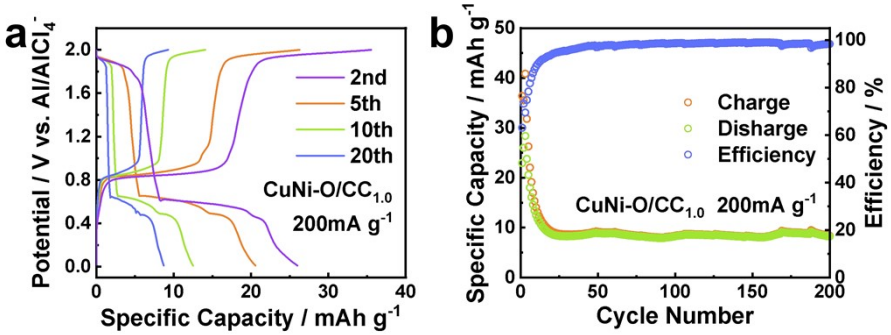

Fig. S10 (a) Charge/discharge curves of CuNi-O/$CC_{1.0}$ cathode for 2nd, 5th, 100th, 200th cycles at a current density of 200 mA g^{-1}. (b) Cycling performance and coulombic efficiency of CuNi-O/$CC_{1.0}$ at a current density of 200 mA g^{-1}.

Table S5. Comparison of metal sulfides as cathode materials for Al batteries.

Active Material	Cathode Preparation	Current Density / mA g^{-1}	Cycle Number	Initial Capacity / mA h g^{-1}	Last Capacity / mA h g^{-1}	Discharge Voltage / V	Loading Mass / mg cm^{-2}
Ni_3S_2/graphene [9]	AM:PTFE=9:1	200	300	235	50	1.0	0.9-1.35
FeS_2 [10]	AM:CF:PTFE=14:5:1	8.94	1	~600	--	0.65	--
SnS_2/graphene [14]	AM:KB:CMC=8:1:1	200	100	392	70	0.68	1.6
NiS [17]	not mentioned	200	100	104.7	104.4	0.9	--
CuS/C [19]	AM:AB:PVDF=6:3:1	20	100	240	90	~1.0	--
VS_2/graphene [20]	AM:AB:PTFE=6:3:1	200	50	165	116	0.7	--
CoS_2 [21]	AM+PVDF	100	100	~130	60	--	--
CoS_2@CNFs [22]	AM:CB:PTFE=7:2:1	200	500	--	~80	--	--
Co_3S_4 [23]	AM:KB:PTEE=8:1:1	50	150	287.9	90	~0.68	1.5
Co_9S_8/CNT-CNF [24]	AM+PS	100	200	315	297	0.95	1.5
WS_2@NCNFs [25]	AM:CB:PVDF=7:2:1	100	100	314.1	195.8	0.6	--
MoS_2 [26]	AM:AB:PVDF=6:3:1	50	100	153.6	112.2	--	--
MoS_2/CNFs [27]	AM+PAN	100	200	293.2	126.6	0.55	~2.2
S-NiCo@rGO [29]	AM:AB:PVDF=6:3:1	1000	100	248.2	83	1.6, 0.9	
This work-powdery Cu-S/Ta	AM:AB:PVDF=6:3:1	200	200	124.2	23.0	1.60, 0.50	0.6
This work-Cu-S/CC	AM+CF	200	200	294.8	30.0	1.75, 0.55	2.2
This work-CuNi-S/$CC_{1.0}$	AM+CF	200	200	333.5	70.5	1.75, 0.85, 0.55	4.2

AM: active material; PVDF: polyvinylidene fluoride; PTFE: polytetrafluoroethylene; KB: ketjen black; CMC: carboxymethyl cellulose; CB: carbon black; PS: polystyrene; AB: acetylene black; CF: carbon fiber